

Sticky Surfaces: Sphere-Sphere Adhesion Dynamics

Sarthok Sircar*, John G. Younger† & David M. Bortz*

*Department of Applied Mathematics, University of Colorado, Boulder, CO 80309

†Department of Emergency Medicine, University of Michigan, Ann Arbor, MI 48109

(Dated: March 27, 2019)

We consider rigid spherical particles coated with binding ligands and study their attachment in quiescent flow. This class of fluid-immersed adhesion is widespread in many natural and engineering settings. Our theory highlights how the physics of the binding kinetics of these ligands (expressed through the collision factor function) as well as the attractive / repulsive surface potential in an ionic medium effects the eventual size of these particle aggregates (flocs). As an application of our theory, we consider a microbial population of spherical bacteria. Our results suggest that the elastic ligands allow large floc aggregates by inducing efficient inter-floc collisions (i.e., a large, non-zero collision factor). Strong electrolytic composition of the surrounding fluid favors large floc formation as well.

PACS numbers:

Introduction – The formation of aggregates, induced by the adhesion of two spherical particles or nearby surfaces is important in many scientific and industrial processes. In particular, interfacial attachment leading to larger floc aggregates via the latching of binders on surfaces in close proximity is widespread. Examples include binding of bacterial clusters to medical implants and host cell surfaces [1], cancer cell metastasis [2], and the coalescence of medical gels with nano-particles for targeted drug delivery [3]. Moreover, coagulation and flocculation (the chemical and the physical aspects of adhesion) are also important in pulp and paper-making industries as well as waste water treatment plants [4]. Although the microscopic structure and geometry of the adhering surfaces of flocs in these phenomena vary greatly, they share a common underlying physics. Past investigations in theoretical modeling of fluid-borne surface adhesion have addressed ligand-receptor binding kinetics [5, 6], surface deformation [7, 8] and flow past the surrounding surfaces [9, 10]. Our aim in this article is to explore how this adhesion (*collision* as termed in the colloid science literature) mechanism for rigid, large (or micron-size), spherical flocs is governed by various geometric and fluid parameters as well as how the surface forces and binding kinetics of the ligands impact the eventual sizes of these flocs. The binder kinetics are significantly different from the core-shell nano-crystal interactions, applicable at a much smaller scale [11, 12]. We consider the sphere-sphere interactions in a quiescent (or no-flow) fluid conditions. The lack of velocity field interactions is an important case from an experimental point of view, e.g., consider the experiments by Sokurenko et al. which studies the catch bond interactions of FimH proteins attached to the rigid surface of *E. coli* in stagnant conditions [13, 14]. Naturally, there are many phenomena in which the hydrodynamics do play a central role and thus the effect of flow-hydrodynamics on floc populations will be a topic for our future work.

Model – Our future studies are geared towards tracking aggregates in suspension, as a continuum mass of EPS (extracellular polymeric substance) network [15]. Following the general outline given in [16], we define

$b(t, x, \mathbf{s})\Delta x$ = number of aggregates having volumes between x & $x + \Delta x$ in time t at a spatial point \mathbf{s} .

In volumes between x_1 and x_2 , the total number of flocs B_0 is given by

$$B_0(t, x_1, x_2, \mathbf{s}) = \int_{x_1}^{x_2} b(t, x, \mathbf{s}) dx \quad (1)$$

for $[x_1, x_2] \subset [\underline{x}, \bar{x}]$, where \underline{x} and \bar{x} are the minimum and maximum aggregate volume sizes, respectively. A finite nutrient supply and the duration of the experiment allow us to assume that \bar{x} is finite. Further, the extracellular structures must be actively maintained and thus the minimal size \underline{x} is the volume of one aggregate. The conservation of the aggregate biomass, or the governing equation for b is [16]

$$b_t + \mathbf{v} \cdot \nabla_{\mathbf{s}} b = A(x, b) \quad (2)$$

where \mathbf{v} is the relative velocity of one floc with respect to the other. $A = A_{\text{in}} - A_{\text{out}}$, where A_{in} is the rate with which flocs of size in $[x, x + \Delta x]$ are created and A_{out} is the rate a floc of size in $[x, x + \Delta x]$ joins with another floc, to form a volume greater than $x + \Delta x$. These rates are given by

$$A_{\text{in}}(x, b) = \frac{1}{2} \int_{\underline{x}}^{x-\underline{x}} K_A(y, x-y) b(t, y, \mathbf{s}) b(t, x-y, \mathbf{s}) dy, \quad x \in [2\underline{x}, \bar{x}] \quad (3a)$$

$$A_{\text{out}}(x, b) = b(t, y, \mathbf{s}) \int_{\underline{x}}^{x-\underline{x}} K_A(x, y) b(t, y, \mathbf{s}) dy, \quad x \in [\underline{x}, x - \underline{x}] \quad (3b)$$

K_A is the aggregation kernel, describing the rate with which flocs of volume x and y combine to form a floc of volume $x + y$. The next two sections will focus on modeling this kernel based on the surface binding kinetics and surface potentials of two coalescing spherical floccules.

Adhesion mechanics – We present a simple model of interfacial attachment between two spheres (of radius R_1 and R_2 , Fig.1) immersed in a fluid medium [5]. The surface of the spheres bind onto each other due to the presence of adherent elastic binders (polymer strands with sticky heads) on the surfaces, as well as the attractive surface potential. The adherent binders are idealized as linear Hookean springs with stiffness κ_0 and mean rest length l_0 (Fig.1). The effect of the shear flow on the mean rest length of the binders, as well as the shearing effect of the mean flow on the binders is neglected [17]. These simplifications allow us to focus on the dynamics normal to the surface, but could be relaxed for a more general case[7].

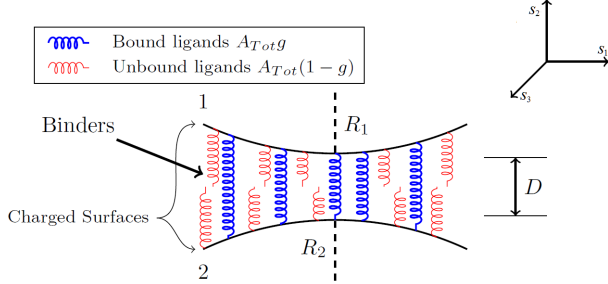


FIG. 1: Two polymer coated coalescing spherical floccules.

For a given spatial point $\mathbf{s} = (s_1, s_2, s_3)$, define $A_{\text{Tot}}g(\mathbf{s}, t)dA$ as the number of bonds in the transverse direction that are attached between the surfaces dA at time t , $D(\mathbf{s})$ be the minimum distance between the two spheres, A_{Tot} be the total number of binding ligands and g be the density of bound ligands on the adhesion surface. In floc literature, the function g is synonymous to the collision factor as well. Hence the total number of bonds formed in the transverse direction is $\int_{A_c} A_{\text{Tot}}g(\mathbf{s}, t)dA$, with A_c being the area of adhesion [5]. The bond attachment/detachment rates, influenced by the surface potential of the two charged surfaces, are

$$\begin{aligned} K_{\text{on}}(\mathbf{s}) &= K_{\text{on}}^* \exp \left[\frac{-\kappa_s(D(\mathbf{s}) - l_0)^2 + W(D(\mathbf{s}))}{2k_B T} \right] \\ K_{\text{off}}(\mathbf{s}) &= K_{\text{off}}^* \exp \left[\frac{(\kappa_0 - \kappa_s)(D(\mathbf{s}) - l_0)^2 + W(D(\mathbf{s}))}{2k_B T} \right] \end{aligned} \quad (4)$$

where k_B is the Boltzmann constant, T is the temperature, κ_s is the spring constant of the transition state used to distinguish catch ($\kappa < \kappa_s$) from slip ($\kappa > \kappa_s$) bonds [5], $W(D)$ is the total surface potential, $K_{\text{on}, \text{eq}}^*$, $K_{\text{off}, \text{eq}}^*$ are the equilibrium binding affinities. For notational simplicity, we denote $D(\mathbf{s}) \equiv D$. In the limit of small binding

affinity and abundant binding receptors on the surface of adhesion ($A_{\text{Tot}}K_{\text{on}, \text{eq}}/K_{\text{off}, \text{eq}} \ll 1$), the bond ligand density evolves as the following differential equation [5]:

$$\frac{dg}{dt} = A_{\text{Tot}}K_{\text{on}} - K_{\text{off}}g, \quad (5)$$

where $\frac{dg}{dt} = \frac{\partial g}{\partial t} + \mathbf{v} \cdot \nabla_s g$. The instantaneous force that these two colliding charged surfaces exert on each other (and acting normal to the surface) becomes:

$$\mathbf{f}(\mathbf{s}, t) = \kappa_0(D - l_0) + \nabla_{\mathbf{D}} \cdot W(D) \quad (6)$$

where the first term represents the stretching force due to Hooke's law and the second term represents the forces due to the surface potential. The direction of this force is along the direction vector from the spherical floc of radius R_1 to the floc of radius R_2 . The total force arising from all such bonds is given by

$$\mathbf{F}(\mathbf{s}, t) = A_{\text{Tot}} \int_{A_c} g(\mathbf{s}, t) \mathbf{f}(\mathbf{s}, t) dA(\mathbf{s}, t) \quad (7)$$

In the limit of small binding affinity and normal adhesion, the adhesion area, A_c , is given by $A_c = \pi R_c^2$ [17], where the adhesion radius, R_c , is

$$R_c(\mathbf{s}, t) = \left(\frac{2k_B T}{\kappa_0} \right)^{1/4} l_0 (R_1^{-1/2}(\mathbf{s}, t) + R_2^{-1/2}(\mathbf{s}, t)) \quad (8)$$

Finally, in a Stokes flow, the aggregation rate, K_A , is

$$K_A = \gamma_A A_c \mathbf{F} / \zeta \quad (9)$$

ζ is the drag coefficient, γ_A is the aggregation contact efficiency parameter. Eqns. (3a, 3b, 2, 5, 6, 7, 9) along with initial conditions, $b(0, x) = b_0(x)$, is the entire system.

Long range interactions – Experiments are being performed to determine the physiochemical characteristics of two coalescing, polymer-coated, charged bacterial floccules immersed in ionic solvents [18]. We describe these interactions through the DLVO approach, i.e., the Coulombic and Van der Waals interaction. To simplify modeling framework, other interactions including hydration effects, hydrophobic attraction, short range steric repulsion and polymer bridging are neglected [19].

For two charged spheres, with radii R_1, R_2 , the repulsive Coulombic forces in the gap, D , is given by

$$W_C(D) = 2\pi\epsilon_0\epsilon\psi_1\psi_2 \left(\frac{2R_1R_2}{R_1 + R_2} \right) e^{-\kappa D} \quad (10)$$

where κ is the Debye length, ϵ, ϵ_0 are the dielectric constant of vacuum and the medium, respectively, ψ_1, ψ_2 are the *zeta potentials* of the respective spheres. The attractive Van der Waals forces for spherical floccules in the regime of close contact ($D \ll R_1, R_2$), is

$$W_{\text{VW}}(D) = -\frac{A}{6D} \frac{R_1R_2}{R_1 + R_2} \quad (11)$$

where A is the Hamaker constant, measuring the van der Waal ‘two-body’ pair-interaction for macroscopic objects. The net surface potential is $W(D) = W_C(D) + W_{VW}(D)$. This potential is pair-wise attractive over very short and long distances, and pair-wise repulsive over intermediate distances (Fig.2).

Results – A number of limitations are imposed in our current approach including hydrodynamic interactions and spatial inhomogeneity arising either through the material parameters or spontaneously (i.e., the variables are independent of the spatial location, \mathbf{s}). The non-equilibrium effects, stochasticity and the discrete number of bonds [1], as well as forces large enough to tear the binding ligands from their anchoring surface [20] are neglected. Further, the binder kinetics is assumed to be independent of the salt concentration (i.e. the spring stiffness, κ_0 is independent of the Debye length, κ). If the adhesion-detachment rate of the flocs is sufficiently rapid so that the time-dependent binding kinetics can be ignored (i.e., we set the term $\frac{\partial g}{\partial t} = 0$ in Eqn.5), then the bond-ligand density (i.e. the collision factor), g , (Eqn. 4, 5) evolves according to

$$g = A_{\text{Tot}} \frac{K_{\text{on}}}{K_{\text{off}}} = \frac{A_{\text{Tot}} K_{\text{on}}^*}{K_{\text{off}}^*} e^{-\kappa_0 \frac{(D-l_0)^2}{2k_B T}}, \quad (12)$$

and the total adhesion force between two flocs reduces to

$$\mathbf{F}(t) = A_{\text{Tot}} g \mathbf{f}[\pi R_c^2(t)] \quad (13)$$

Surface potential and collision factor – The pair-wise surface potential, $W(D)$, is valid over short distances ($D \ll R_1, R_2$). The salt dissolved in the fluid is assumed to be a 1-1 electrolyte at different concentrations, zeta potentials and Debye lengths, listed in Table I, and used from Camesano’s experiments involving adhesion of rigid spherical bacterial surface with silicon nitride AFM tip [21], while the calculation of the Debye length from different electrolyte concentration is given in [22] (Chap-14). The dielectric constant in vacuum is $\epsilon_0 = 8.854 \times 10^{-12}$, while the permittivity of water at $T=25^\circ\text{C}$ is $\epsilon = 78.5$.

[salt] (M)	ψ_1 (mV)	ψ_2 (mV)	κ
0.01	-16	-31.7	3.04
0.05	-14	-9.2	1.36
0.5	-10	-3	0.43

TABLE I: Parameters corresponding to DLVO interactions [21].

A weak electrolytic solution (e.g., $\kappa = 3.04$ curve, Fig. 2a) has a large potential energy barrier at short separation distances, since a weak salt solution results in diffuse screening length surrounding the charged surfaces which hinders adhesion (see the floc population studies in Fig. 4a). Conversely, for sufficiently concentrated solution (e.g., $\kappa = 0.43$ curve, Fig. 2a), the energy barrier

disappears and aggregation is favored. The primary minima (shown in Fig. 2a) is unphysical, since at very short separation distances the non-DLVO repulsive steric interaction is dominant that prevents the particles from coming into true contact. The regions of attraction/repulsion of this potential is inferred from surface force per binder, \mathbf{f} (Fig. 2b). For sufficiently concentrated salt solution these forces are attractive ($\mathbf{f} > 0$ for all \mathbf{D} , $\kappa = 0.43$ curve, Fig. 2b) and hence, always favor adhesion. Otherwise, at intermediate distances ($2\text{nm} < D < 15\text{nm}$), the repulsive Coulombic forces are dominant while at longer distances ($D > 15\text{nm}$), the adhesive forces are dictated by the attractive spring force of the stretched binders. We choose to conduct our numerical simulations at $D^* = 11\text{nm}$, where the adhesive forces are attractive.

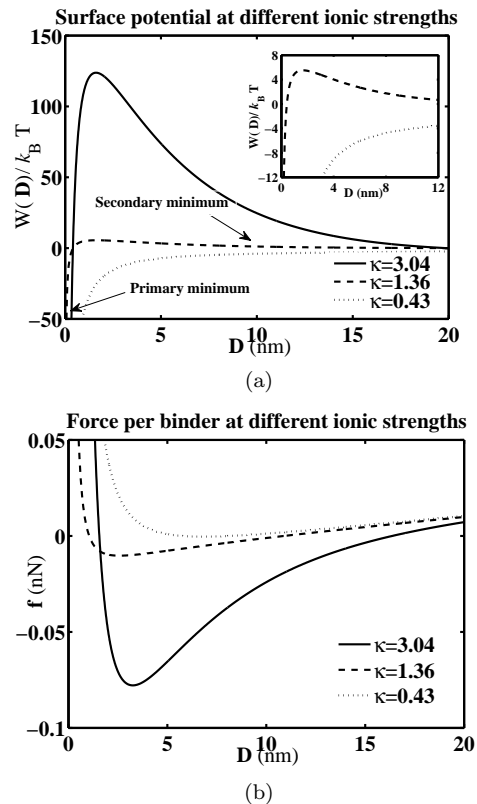


FIG. 2: (a) Total surface potential, $W(\mathbf{D})$ versus the separation distance \mathbf{D} , for two rigid, spherical flocs of radii $R_1 = 0.25\mu\text{m}$ and $R_2 = 0.5\mu\text{m}$ respectively, and (b) surface force per binder, \mathbf{f} , (Eq. 6) versus \mathbf{D} ; at different ionic concentration of a 1:1 electrolyte. Regions of attraction: $\mathbf{f} > 0$, region of repulsion: $\mathbf{f} < 0$.

The collision factor, $g(D)$, (where the separation distance, $D = \frac{s_1^2 + s_2^2}{R} + l_0$, with the center of the spatial frame, located at the point of minimum separation, and on the surface of sphere 2, R being the radius of two identically colliding flocs, see Fig.1) is symmetric about the mean rest length of the binders, l_0 , in the absence of fluid flow (Fig.3). Since the floc separation distance with a significant non-zero contact is considerably reduced for stiff

binders, the adhesion-detachment mechanism is more efficient for tensile springs (e.g., compare the non-zero region in Fig. 3a vs. Fig. 3b).

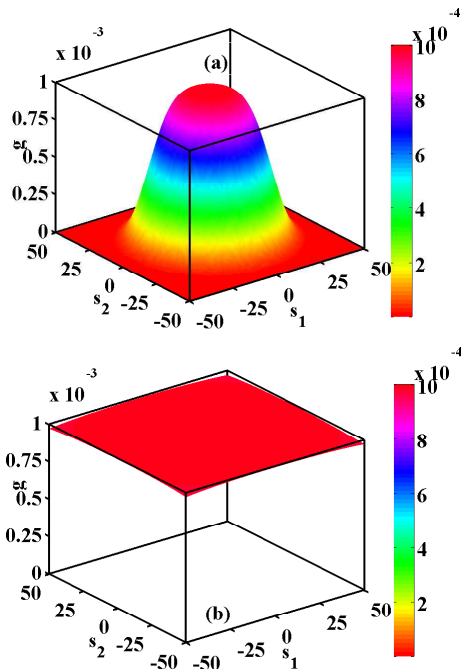


FIG. 3: Collision factor g vs spatial coordinates (s_1, s_2) with (a) $\kappa_0 = 10^{-2} \text{ Nm}^{-1}$ and (b) $\kappa_0 = 10^{-5} \text{ Nm}^{-1}$. Stiff ligands have a narrow range of separation distance $D(s_1, s_2)$ with a non-zero collision impact. The plane (s_1, s_2) separates the two spheres with the origin located at the point of minimum separation and on the surface of sphere 2.

Numerics – To solve the complete population model using the adhesion kernel described through the binder kinetics above, we employed the discretization scheme developed by Banks et. al. [23, 24] and adopted by Doumic [25]. The parameters used in the simulations are listed in Table II.

Parameter	Value	Units	Source
κ_0	$(0.01-10) \times 10^{-3}$	N m^{-1}	[17]
l_0	10^{-8}	m	[17]
ζ	(0.01-2.5)	$\text{N m}^{-1} \text{ s}$	–
A_{Tot}	10^9	m^{-2}	[17]
$K_{\text{on}}^*/K_{\text{off}}^*$	10^{-12}	–	[17]
γ_A	2.7×10^{-15}	fL^{-2}	[16]
A	$2.44k_B T$	J	[19]

TABLE II: Parameters common to all simulations.

The convergence of the scheme was tested using the test functions in [16]. A linear relationship between the L^∞ -error and the mesh-size, δx was found using this first order approximation scheme. The initial number density is chosen as $b_0(x) = 7.47 \times 10^{-4} e^{-0.00676x}$, where the coefficients are fit to the experimental data from the Younger Lab [16]. All solutions are marched in time until $T=100$ minutes. We chose 1 femtoliters (fL) as a lower bound

\underline{x} in our simulations. Our aggregation model allows the upper bound, \bar{x} , of the domain to go unrestrained (i.e., $\bar{x} \rightarrow \infty$), but the results are presented inside the window $1 \leq x \leq 1000 \text{ fL}$.

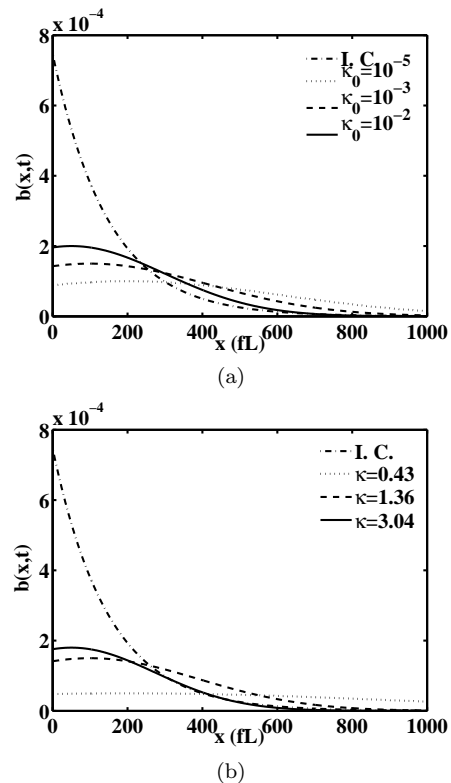


FIG. 4: Floc number density distribution versus floc-volume at time $T=100 \text{ min}$ for (a) different binder stiffness and screening length, $\kappa = 1.5$, and (c) different screening lengths and $\kappa_0 = 10^{-3} \text{ Nm}^{-1}$. The dash-dot curve in these figures is the initial conditions ($b_0(x)$).

Fig. 4 highlights the floc population at different surface parameter, κ_0 , and fluid parameter, κ . These studies suggest that stiff binders lead to fewer large aggregates (i.e., $b(x, T, \kappa_0 = 10^{-2}) < b(x, T, \kappa_0 = 10^{-3}) < b(x, T, \kappa_0 = 10^{-5})$, for $x \geq 600$). This is not surprising since aggregation is influenced by the collision factor (see Eq. 9, 13). A higher value of $g(D^*)$ suggests that two flocs close to each other are more likely to coalesce leading to bigger flocs. However, at a separation distance, $D^* = 11 \text{ nm}$ used in our numerical simulations, this factor is insignificant for stiff binders (e.g. compare the values of $g(D^*)$ in Fig. 3a vs. Fig. 3b) and does favor formation of large aggregates. Surface-adhesion is comparatively stronger in highly ionic fluids, represented by a shorter Debye length, κ . A short screening length implies a smaller separation distance between the interacting surfaces, and hence a strong adhesion (Fig. 4b). Similarly, we have found that adhesion is favorable among flocs of smaller sizes (i.e., smaller radius of the coalescing spheres). This is effect is due to a smaller sphere-sphere potential energy barrier. *Conclusion* – We consider rigid, spherical flocs of size one

micron and larger and present a basic floc aggregation model under the influence of a surface potential. We investigate the implications of our model in terms of a *collision factor*, which is a factor widely used in the engineering literature [4]. Predictions about the floc aggregate size, at various fluid and surface potential parameters, are also made using numerical simulations. Preliminary investigation in quiescent flow conditions reveals that the adhesion mechanism is favored if the binding ligands of the flocs are elastic, or the surrounding fluid is highly ionized, or the size of the aggregating flocs are small.

Acknowledgment: This work supported by grants NSF 1225878 and NIH 1R01GM081702-01A2.

-
- [1] C. Zhu, *Journal of Biomechanics* **33**, 23 (2000).
- [2] X. Lei, M. B. Lawrence, and C. Dong, *J. Biomech. Eng.* **121**, 636 (1999).
- [3] N. W. Moore and T. L. Kuhl, *Biophys. J.* **91**, 1675 (2006).
- [4] P. Somasundaran, V. Runkanan, P. Kapur, H. Stechemesser, and B. Dobiáš, in *Coagulation and Flocculation* (Taylor & Francis, 2005), vol. 126, chap. 11, pp. 767–803, 2nd ed.
- [5] M. Dembo, D. C. Torney, K. Saxman, and D. Hammer, *Proc. Royal Soc. B* **234**, 55 (1988).
- [6] G. Bell, *Science* **200**, 618 (1978).
- [7] S. Reboux, G. Richardson, and O. Jensen, *Proc. Royal Soc. A* **464**, 447 (2008).
- [8] E. A. Evans, *Biophys. J.* **48**, 175 (1985).
- [9] A. Goldman, R. Cox, and H. Brenner, *Chemical Engineering Science* **22**, 637 (1967).
- [10] M. R. King and D. A. Hammer, *Biophys. J.* **81**, 799 (2001).
- [11] J. F. L. Duval, J. P. Pinheiro, and H. P. van Leeuwen, *The Journal of physical chemistry. A* **112**, 7137 (2008).
- [12] P. Reiss, M. Protière, and L. Li, *Small* **5**, 154 (2009).
- [13] E. V. Sokurenko, V. Chesnokova, R. J. Doyle, and D. L. Hasty, *The Journal of biological chemistry* **272**, 17880 (1997).
- [14] E. V. Sokurenko, V. Chesnokova, D. E. Dykhuizen, I. Ofek, X. R. Wu, K. a. Krogfelt, C. Struve, M. a. Schembri, and D. L. Hasty, *Proceedings of the National Academy of Sciences of the United States of America* **95**, 8922 (1998).
- [15] E. C. Byrne, S. P. Dzul, M. J. Solomon, J. G. Younger, and D. M. Bortz, *Physical Review E* **83**, 41911 (2011).
- [16] D. M. Bortz, T. L. Jackson, K. A. Taylor, A. P. Thompson, and J. G. Younger, *Bull. Math. Biology* **70**, 745 (2008).
- [17] M. Mani, A. Gopinath, and L. Mahadevan, *Physical Review Letters* **108** (2012).
- [18] S. Camprubí, S. Merino, J. Benedí, P. Williams, and J. M. Tomás, *Current Microbiology* **24**, 31 (1992).
- [19] J. Gregory, *Particles in Water* (CRC Press, 2006).
- [20] M. Varenberg and S. Gorb, *Journal of The Royal Society Interface* **4**, 721 (2007).
- [21] N. I. Abu-Lail and T. a. Camesano, *Biomacromolecules* **4**, 1000 (2003).
- [22] J. Israelachvili, *Intermolecular and Surface Forces* (Academic Press, Amsterdam, 2011), 3rd ed.
- [23] H. T. Banks and F. Kappel, *Semigroup Forum* **38**, 141 (1989).
- [24] A. S. Ackleh and B. G. Fitzpatrick, *J. Math. Biology* **35**, 480 (1997).
- [25] S. Prigent, A. Ballesta, F. Charles, N. Lenuzza, P. Gabriel, L. M. Tine, H. Rezaei, and M. Doumic, *PLoS ONE* **7**, e43273 (2012).